Journal of Magnetic Resonance 206 (2010) 68–73

Contents lists available at ScienceDirect

Journal of Magnetic Resonance

journal homepage: www.elsevier.com/locate/jmr

An alternative scheme for the multiplexed acquisition of 1D and 2D NMR spectra

B. Plainchont [a], A. Martinez [a], S. Tisse [b], J.-P. Bouillon [b], J.-M. Wieruszeski [c], G. Lippens [c], D. Jeannerat [d], J.-M. Nuzillard [a,*]

[a] Institut de Chimie Moléculaire de Reims, Université de Reims Champagne-Ardenne, CNRS UMR 6229, BP 1039, F-51687 Reims Cedex 2, France
[b] Sciences et Méthodes Séparatives, I.R.C.O.F., Université de Rouen, UPRES EA 3233, F-76821 Mont-Saint-Aignan Cedex, France
[c] Groupe RMN et Modélisation moléculaire, Université des sciences et technologies de Lille, CNRS UMR 8576, F-59655 Villeneuve d'Ascq Cedex, France
[d] Département de Chimie Organique, Université de Genève, 30, quai Ernest Ansermet, CH-1211 Genève 4, Switzerland

ARTICLE INFO

Article history:
Received 22 April 2010
Revised 3 June 2010
Available online 9 June 2010

Keywords:
Multiplexed acquisition
Hadamard spectroscopy
Shaped pulses
TOCSY
COSY
HSQC
Cyclodextrin derivatives

ABSTRACT

Spin system selective 1D ^{1}H, 2D DQF-COSY and 2D HSQC NMR spectra were recorded in order to fully assign the ^{1}H and ^{13}C 1D NMR spectra of an asymmetrical β-cyclodextrin derivative. Instead of individually accessing the seven sugar anomeric protons by means of long multiplet selective pulses, only short region selective pulses were used. The simultaneously selected anomeric protons were differentiated by allowing their magnetization to evolve under the sole effect of the chemical shift interaction. In each experiment, the seven recorded spectra were linear combinations of the seven desired ones. The combination coefficients were measured and used to obtain almost perfectly separated sugar unit sub-spectra. This multiplexed acquisition scheme resulted in a time gain factor of about 2.

1. Introduction

A 2D NMR spectrum can be considered as series of 1D spectra in which the amplitude or the phase of peaks is modulated as a function of evolution time t_1. The Fourier transformation in the indirect dimension unscrambles these modulations, so that each 1D spectrum participates in the signal-to-noise ratio of the final result [1]. An alternative to the introduction of an additional dimension is the use of selective radiofrequency pulses [2]. A full 2D NOESY spectrum can be replaced by a small number of 1D NOESY spectra that concentrate on the resonances of interest by means of their selective excitation. However, the sequential recording of 1D spectra is not the most efficient approach with respect to the signal-to-noise ratio that can be obtained within a given spectrometer occupancy time. The selective pulse approach can benefit from the same advantage as 2D NMR if n independent 1D acquisitions are replaced by n multiplexed acquisitions in which each desired spectrum is present but in variable proportions. Like FT, the unscrambling operation is equivalent to the computation of n linear combinations of the n acquired spectra. The procedure may result in an overall signal-to-noise improvement if the combination coefficients are adequately chosen. The most popular implementation of such a strategy is known as Hadamard spectroscopy [3].

The success of a Hadamard NMR spectroscopy experiment depends on the ability to simultaneously and selectively act on individual resonances or on groups of resonances so that some of them appear with positive amplitudes and others with negative ones [4–7]. In other words, the scrambling process is described by an $n \times n$ matrix that contains only 1 and -1 elements [8].

The following sections describe an alternative to Hadamard encoding that also provides amplitude modulated mixtures of individual spectra. The method is well adapted to the analysis of oligosaccharides and was used to assign the resonances of a chemically modified β-cyclodextrin. In this detailed example, the low dispersion of the chemical shifts of the anomeric protons would have required very long soft pulses to correctly set up the Hadamard encoding scheme.

2. Principle

Molecules such as oligosaccharides contain many ^{1}H spin systems whose signals overlap, thus making spectral interpretation difficult [9]. When an-om-er-ic proton signals are sufficiently separated, their individual selective excitation is feasible. The

* Corresponding author. Fax: +33 3 26 91 35 96.
E-mail addresses: bertrand.plainchont@etudiant.univ-reims.fr (B. Plainchont), agathe.martinez@univ-reims.fr (A. Martinez), severine.tisse@univ-rouen.fr (S. Tisse), jean-philippe.bouillon@univ-rouen.fr (J.-P. Bouillon), Jean-Michel.Wieruszeski@univ-lille1.fr (J.-M. Wieruszeski), guy.lippens@univ-lille1.fr (G. Lippens), Damien.Jeannerat@unige.ch (D. Jeannerat), jm.nuzillard@univ-reims.fr (J.-M. Nuzillard).

1090-7807/$ - see front matter © 2010 Elsevier Inc. All rights reserved.
doi:10.1016/j.jmr.2010.06.005

magnetization transfer from an anomeric ^{1}H nucleus to its whole spin system by isotropic mixing opens the way to various experiments that bring information about that spin system [10,11]. The set of all individual sub-spectra that can be obtained in this way for a molecule of interest is collectively referred to as "the source" and is formally represented by a $p \times n$ matrix in which p is the number of spectral points and n is the number of sources. More precisely, the S source matrix is the theoretical one that would be recorded if the spectrometer did not add noise to signals and if there were no signal loss due to the selective excitation (or inversion, or refocusing) process. The experimental data matrix Y_0 is therefore

$$Y_0 = S + N_0 \tag{1}$$

in which N_0 represents the noise of the set of non multiplexed spectra.

In multiplexed experiments, the recorded data Y is represented by

$$Y = S \cdot A + N \tag{2}$$

in which A is the mixing matrix and N a noise matrix that is different from N_0 but shares the same properties. The noise has a zero mean, it is uncorrelated between two different spectra and its standard deviation σ_0 is the same in all spectra. The elements of A are subjected to the condition $|A_{ij}| \leqslant 1$ because the multiplexing process cannot create magnetization. However, $|A_{ij}|$ values should be as close as possible to 1 in order to reduce the influence of noise on the acquired data. Matrix A must also be invertible, so that an estimate $\widehat{S}$ of the sources can be retrieved from the experimental values in Y using

$$B = A^{-1}$$
$$\widehat{S} = Y \cdot B$$
$$\text{so that} \quad \widehat{S} = S + N \cdot B \tag{3}$$

A simple calculation shows that the standard deviation of the noise in the jth estimated source (column j in $\widehat{S}$) is given by

$$\sigma_j = \sigma_0 \sqrt{v_j} \tag{4}$$

$$\text{with} \, v_j = \sum_{k=1}^{n} B_{kj}^2 \tag{5}$$

A good mixing scheme yields v_j elements in the v row vector that are as small as possible. The time gain G that is achieved by running n multiplexed acquisitions instead of the n separated acquisitions that would lead to the same spectral signal-to-noise ratio is given by

$$G = \frac{1}{n} \sum_{j=1}^{n} \frac{1}{v_j} \tag{6}$$

Considering H_4, the Hadamard mixing matrix for $n = 4$, then

$$A = \begin{vmatrix} 1 & 1 & 1 & 1 \\ 1 & 1 & -1 & -1 \\ 1 & -1 & 1 & -1 \\ 1 & -1 & -1 & 1 \end{vmatrix}$$
$$B = \frac{1}{4} A$$
$$v = \frac{1}{4} |1 \quad 1 \quad 1 \quad 1|$$
$$\sigma_j = \frac{\sigma_0}{2} \quad 1 \leqslant j \leqslant 4$$
$$G = 4.$$

The factor of 2 in the signal-to-noise ratio that is gained by adding and subtracting four spectra in all possible ways is equivalent to a time gain by a factor of 4.

A good multiplexing scheme is one in which the columns in A are as linearly independent as possible. The determinant of matrix A is zero when at least one of the mixed spectra is a combination of the others, thus making it impossible to retrieve the n sources from the n mixtures. For a given n value, multiplexing is the most efficient when $|\det(A)|$ is the highest. The G and $\det(A)$ values are global independence indicators while the elements in v give direct information about the noise amount in each separated spectrum.

Fig. 1 shows the structure of compound **1**, its 500 MHz ^{1}H NMR spectrum and an expansion of the anomeric protons. Our interest in this molecule came from its use in the synthesis of new efficient stationary phases for gas chromatographic applications [12]. The seven sugar spin systems were labeled A–G, according to the order of appearance of their anomeric protons. The ^{1}H NMR spectrum is dominated by the nineteen methoxy singlet signals that superimpose with sugar ^{1}H resonances. A clean selective excitation or inversion of individual anomeric doublets leaving the neighboring resonances untouched would require hundreds of ms long selective pulses. The extensive relaxation during such long pulses prompted us to use "offset encoding".

The pulse sequence in Fig. 2a shows the implementation of our approach. It was applied to record 1D ^{1}H, 2D DQF-COSY and 2D HSQC spectra of the seven spin systems of **1**. This is basically a TPPI 2D experiment in which t_1 is incremented in $\Delta t_1 = 1/(2SW_1)$ steps while ϕ_1 is incremented in $\pi/2$ steps [13]. Phase ϕ_1 starts at $\pi/2$ and t_1 at Δt_1. Only the first seven FIDs are recorded ($n = 7$):

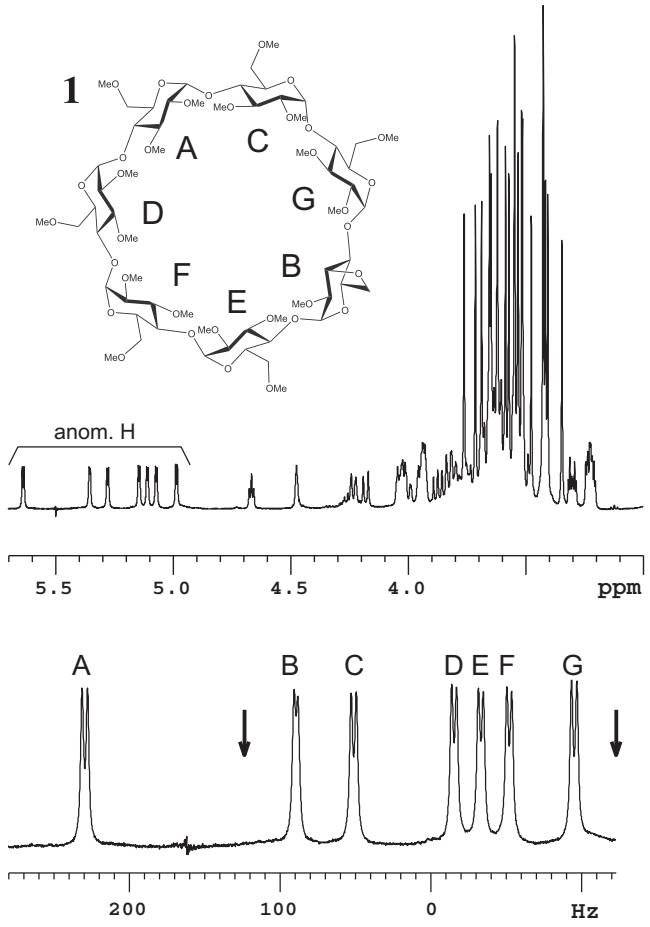

Fig. 1. The structure of compound **1** and its ^{1}H NMR spectrum. The origin of the frequency scale in the zoomed anomeric region (bottom) was set to the position of the carrier frequency ν_0. The two arrows mark the limits of the SW_1 wide frequency range that define the value of the t_1 increment (see Fig. 2 and text).

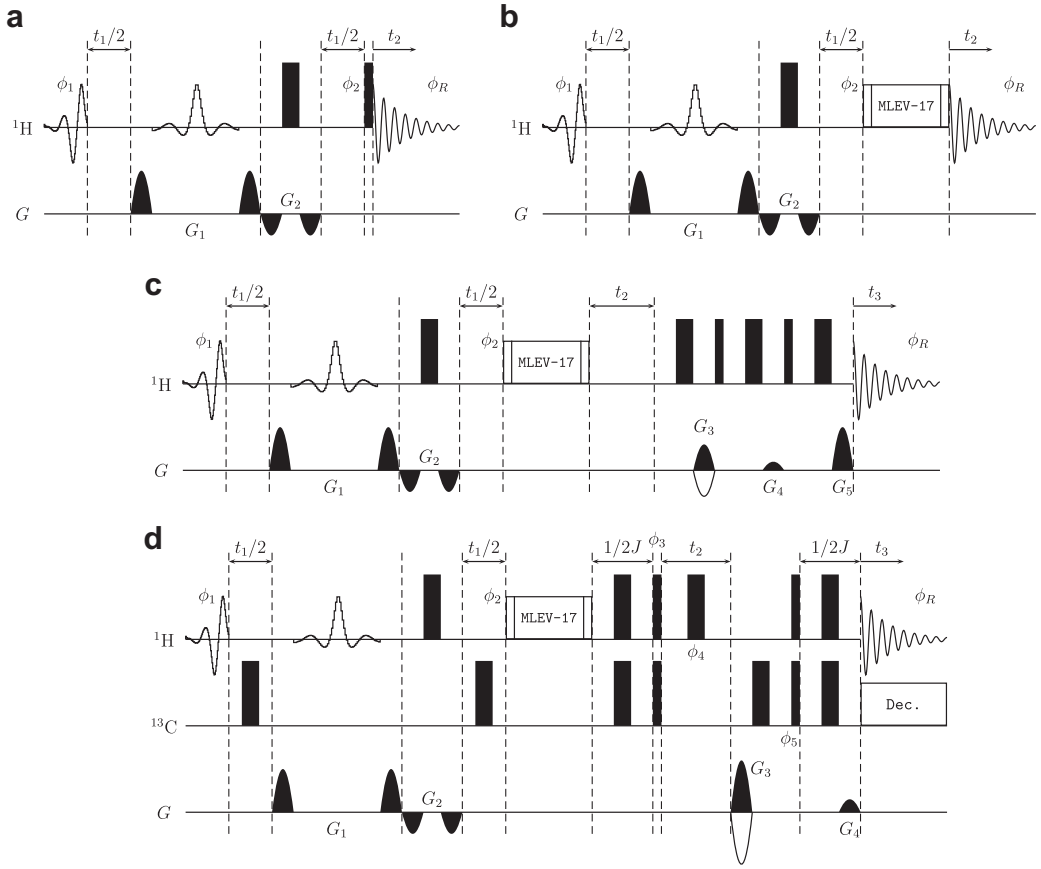

Fig. 2. Pulse sequences for multiplexed spectra acquisition using offset encoding. The narrow and wide black boxes stand for hard $\pi/2$ and π pulses (25 kHz intensity) of x phase, unless otherwise specified. The phase of the first soft pulse (E-BURP-2, 10 ms) and the value of t_1 are varied according to Eq. (7). Gradient intensity values are provided in captions of Figs. 3–6 as percents of the hardware dependent maximum intensity (50 G/cm). All gradient pulses are 0.5 ms long. MLEV-17 (200 ms) and trim pulses (2 ms) are emitted at a 8 kHz intensity. The receiver phase is kept constant upon alternation of ϕ_2 ($\pm x$) and inverted when the phase of the soft refocusing pulse is varied in $\pi/2$ steps. (a) The basic sequence that permits an experimental determination of how the desired spectra are mixed. (b) The multiplexed 1D-TOCSY sequence. (c) The multiplexed 2D-TOCSY-DQF-COSY sequence. (d) The multiplexed 2D-TOCSY-HSQC sequence. The hard ^{13}C π pulses in the middle of the $t_1/2$ delays cancel the action of heteronuclear couplings during t_1.

$$t_1 = j\Delta t_1 \quad \text{and} \quad \phi_1 = j\frac{\pi}{2} \quad (1 \leqslant j \leqslant n) \tag{7}$$

The two selective pulses in sequence 2a have the same operation frequency band and therefore the effect of the chemical shift of the nuclei they act on is preserved during t_1 because the two refocusing pulses mutually cancel for these nuclei. The couplings with the partners located outside the inverted region are refocused during the second half of the t_1 evolution time. In the present case, the anomeric proton magnetization evolves as if it were decoupled during t_1. The soft and hard inversion pulse combination was already proposed by Ernst and coworkers [14] and used by others [15,16] for the recording of F_1 decoupled semi-selective homonuclear 2D spectra, but without gradient enhancement. The gradient pulses make it possible to eliminate the phase cycling of the refocusing pulses and provide spectra that are as clean in a single scan as those obtained with a 16 step phase cycle. This feature is particularly useful for the study of compound **1** because the strong signals of the methoxy group are difficult to eliminate from a region with the important low-amplitude signals of the carbohydrate. A detailed analysis shows that the couplings operate only during the two G_2 gradient pulses. Their effect is negligible considering the homonuclear ^{1}H coupling intensities and the usual gradient pulse lengths.

A simple analysis of the pulse sequence in Fig. 2a shows that the intensity of the signal of a nucleus I_k of offset frequency Ω_k is modulated by a factor

$$F_k = \sin(\phi_1 - \Omega_k t_1). \tag{8}$$

The last hard pulse in sequence 2a produces the desired amplitude modulation of the signal of I_k; its removal would lead to phase modulation of the signal. The dependence of signal intensities on offset values justifies the name "offset encoding" that was given to our approach. Of course, the soft pulses must not introduce any offset-dependent phase and amplitude modulations over their effective bandwidth. Considering that ϕ_1 and t_1 are chosen according to Eq. (7), the modulation factor of the kth peak in the jth spectrum is given by

$$F_{kj} = \sin(j(\pi/2 - \Omega_k \Delta t_1)) \tag{9}$$

resulting in the mixing coefficient

$$a_{kj} = R_{kj} F_{kj} \tag{10}$$

in which R_{kj} is a factor taking into account the relaxation of nucleus I_k during t_1 and the soft pulses, and eventually other sources of experimental errors.

For the anomeric ^{1}H signals in compound **1**, the seven FIDs ($1 \leqslant j \leqslant 7$) yield seven spectra in which the peak amplitude modulation law (relaxation effect excluded) of the seven anomeric signals ($1 \leqslant k \leqslant 7$) is known once the carrier frequency and the SW_1 sampling rate are chosen.

The TPPI procedure that is proposed for the variation of t_1 and ϕ_1 according to j is only an option among many others. It is suggested here only because it is very simple to implement, as

any ordinary TPPI 2D experiment. The operation conditions, namely the ϕ_1 phases and the associated t_1 delays, may however be chosen in other ways. The criterion for the selection of a good set of acquisition parameters is quite simple: the elements in vector v should be as small as possible and therefore G should be as large as possible. As relaxation factors in matrix R are not easy to predict and cannot be neglected, a good approach for the evaluation of matrix A is to use the sequence 2a and to integrate the n signals of interest in the n mixed spectra. The resulting estimation $\widehat{A}$ of A must be scaled so that its elements satisfy $|\widehat{A}_{ij}| \leqslant 1$. Dividing the matrix of peak integrals by its highest value achieves this goal but may result in an over-estimation of A and therefore in an over-estimation of the time gain G, in the case where no element in A is close to 1 or -1. The estimation of the source spectra $\widehat{S}$ is then simply obtained from the acquired multiplexed spectra in matrix Y by computing $Y \cdot \widehat{A}^{-1}$.

The logic of pulse sequence 2a was also extended to the TOCSY experiment sequence (see Fig. 2b). In sequence 2b the magnetization of the initially excited nuclei evolves during t_1 and only the component along the x axis of the rotating frame is transferred by isotropic mixing to the rest of the spin system. The trim pulses in sequence 2b play the same role as the last hard pulse in sequence 2a, as they create the desired signal amplitude modulation. When carried out with identical variations of ϕ_1 and t_1, sequences 2a and 2b should result in identical mixing and separation matrices. An $\widehat{A}$ matrix can also be directly obtained by integration of the initially excited peaks in the mixed 1D-TOCSY spectra.

Sequence 2b was extended to 2D-TOCSY-DQF-COSY and 2D-TOCSY-HSQC experiments (see Fig. 2c and d). These sequences have already been reported for the analysis of complex oligosaccharides but without multiplexed acquisition [17,18]. Many more interesting applications can be envisaged. The 1D-TOCSY preparation period makes it possible to transform any 2D-X experiment (X = COSY, NOESY, J-resolved, HSQC) into the corresponding selective 2D-TOCSY-X experiment according to a well-established procedure [10]. Sequences 2c and 2d are implemented as regular 3D experiments with n t_1 increments, in the TPPI mode for the first indirect (multiplexed) dimension and in echo/antiecho mode in the second indirect dimension. The n F_2/F_3 planes that are obtained by FT along the t_2 and t_3 time axes yield the n separated 2D spectra after their separation by matrix $\widehat{B}$. This particular data processing step characterizes the difference between a regular 3D NMR approach and offset encoding. In the case of HSQC spectra, the integration of the generally well separated 2D peaks provides the best evaluation of $\widehat{B}$. Direct integration is however not possible for DQF-COSY spectra because all peak clusters have a null volume due to their anti-phase nature. In this case, the $\widehat{B}$ matrix that derives from sequence 2a can be used.

3. Results and discussion

The offset encoding method was exemplified with compound **1** and its set of seven anomeric ^{1}H resonances (Fig. 1). The resonances D, E and F being separated by a mere 18 Hz (see Fig. 1), they could not cleanly be addressed by Hadamard-type encoding. Offset encoding was a very attractive alternative.

All spectra were recorded on a 500 MHz DRX Bruker spectrometer fitted with an inverse detection probehead. The sample was dissolved in $CDCl_3$ at a 20 mM concentration. In all experiments the first excitation pulse was a 10 ms long E-BURP-2 that covered 400 Hz [19]. It was frequency shifted by 48 Hz to avoid the unwanted excitation of the most deshielded non anomeric proton. The soft refocusing pulse was a 10 ms long RE-BURP that was also frequency shifted by 48 Hz. BURP pulses were chosen because they ensure a high level of amplitude and phase uniformity over their effective bandwidth.

All spectra in Figs. 3–6 were recorded in the same conditions regarding the choice of the ν_0 RF carrier frequency and of SW_1. These two parameters have a strong impact on the sensitivity enhancement that is expected from multiplexing and were chosen to maximize $|\det(A)|$. Qualitatively, if SW_1 is too large (Δt_1 too small) all of the sine-modulated ($\phi_1 = 0$ or π) spectra and cosine-modulated spectra ($\phi_1 = \pm\pi/2$) will be similar, thus resulting in a barely separable spectra set. If SW_1 is too small (smaller than the width of the region that contains the anomeric resonances) there will be some evolution frequency folding, due to the periodic nature of the sine function in Eq. (9). If two resonances have identical or nearly identical apparent evolution frequencies their behavior during t_1 will be indistinguishable, thus leading to poor separability. We chose to fold resonance A in the middle of the space between resonances B and C. This defined $\nu_0 + SW_1/2$ because folding occurs in TPPI mode around the boundaries of the spectral region. Then, $\nu_0 - SW_1/2$ was adjusted so that the theoretical $|\det(A)|$ was maximum. The position of the $\nu_0 \pm SW_1/2$ spectral

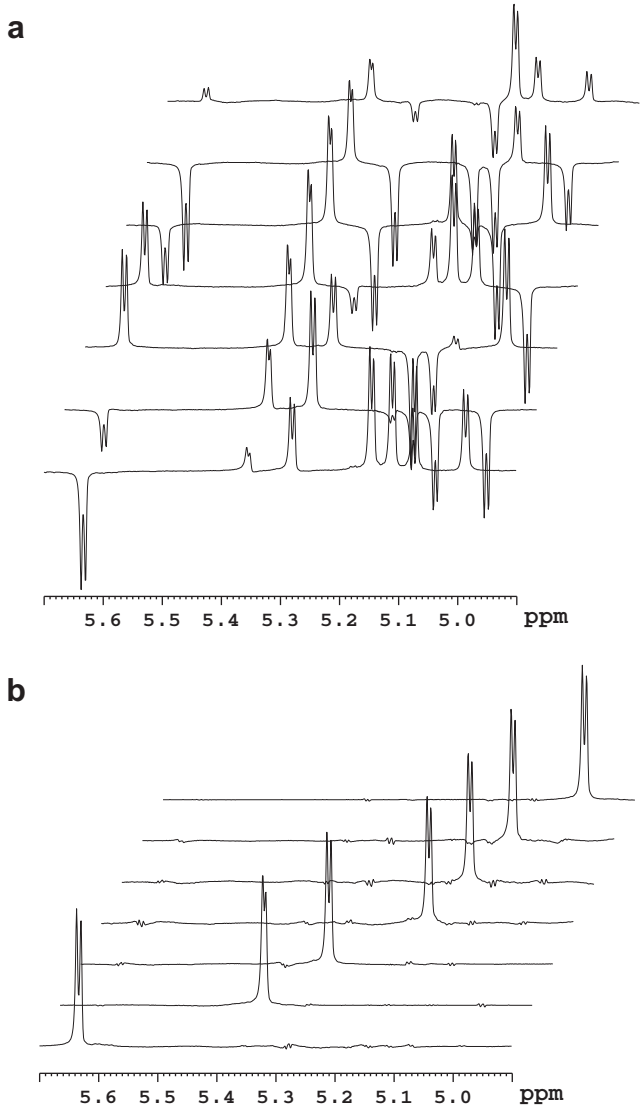

Fig. 3. (a) The mixed anomeric signals from sequence 2a. G_1/G_2 = 30/−10. Acquisition time was 2.3 min (8 transients per t_1 value). (b) The separated anomeric signals that were obtained from the mixtures in Fig. 3a. The mixing matrix $\widehat{A}$ (see text) was obtained by integration of the seven doublets in each spectrum.

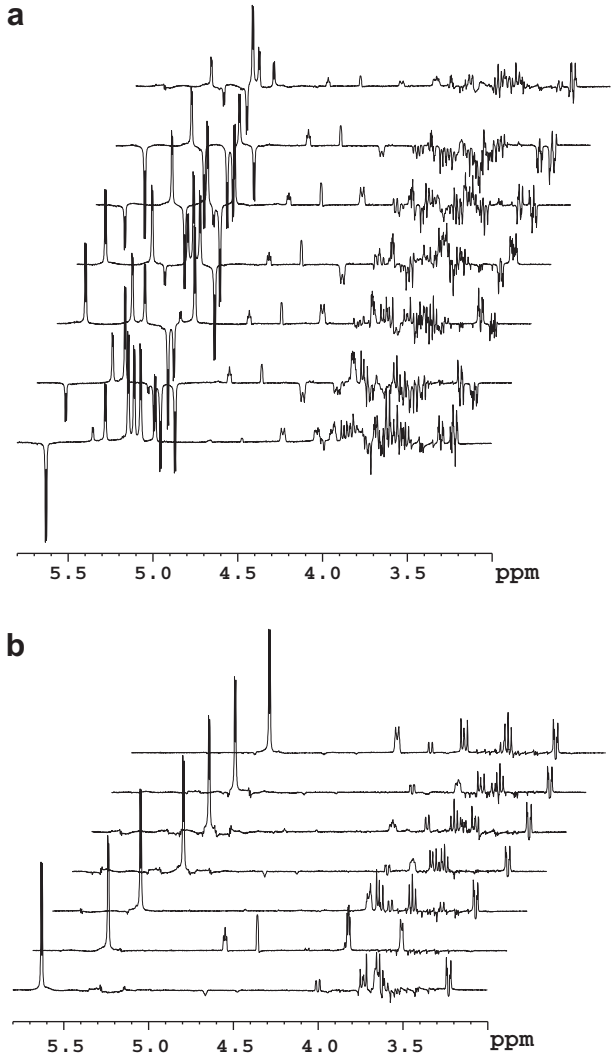

Fig. 4. (a) The mixed 1D-TOCSY signals from sequence 2b. G_1/G_2 = 30/−10. Acquisition time was 4.9 min (16 transients per t_1 value). (b) The separated 1D-TOCSY spectra of the anomeric protons that were obtained from the mixtures in Fig. 4a, when processed as spectra in Fig. 3b.

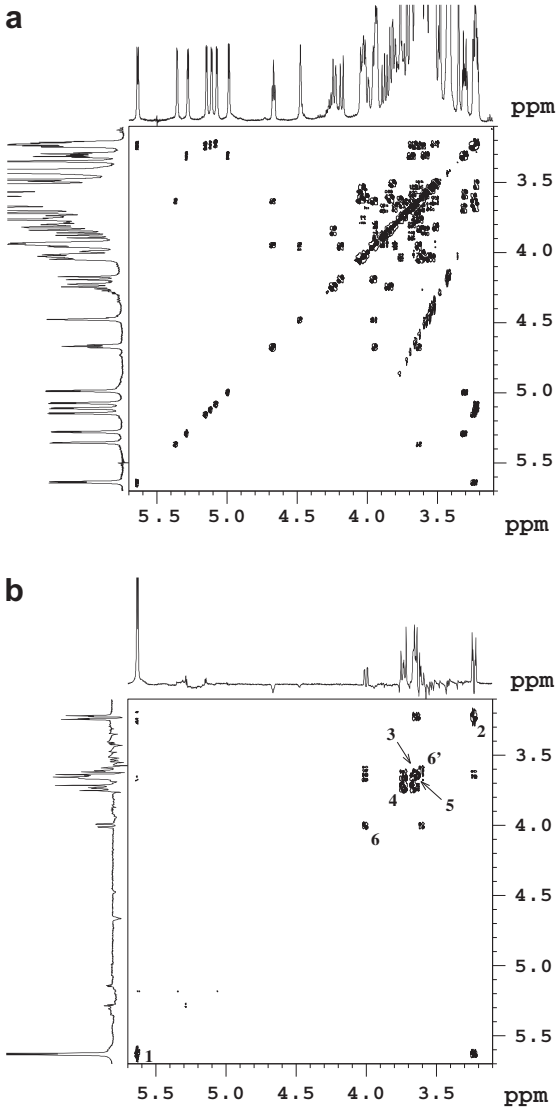

Fig. 5. (a) The DQF-COSY spectrum of compound **1**. (b) The 2D-TOCSY-DQF-COSY of sugar unit A. The complete set of 2D-TOCSY-DQF-COSY spectra was obtained in 14 h and 18 min (eight transients per t_1 value, 512 t_2 values). $G_1/G_2/G_3/G_4/G_5$ = 40/−15/±30/10/50. Separation was achieved as for spectra in Figs. 3 and 4b.

limits are marked by arrows in Fig. 1. The optimal SW_1 value was 246 Hz, so that Δt_1 was 2.033 ms. The maximum t_1 value was therefore 14.228 ms, to which two times 10 ms (for the two soft pulses) must be added, thus leading to less than 35 ms between the beginning of the pulse sequence and the end of the encoding step. The theoretical v_{th} vector was

$$v_{th} = |\,0.35 \quad 0.29 \quad 0.31 \quad 0.70 \quad 0.90 \quad 0.59 \quad 0.25\,| \tag{11}$$

and resulted in G_{th} = 2.55, under the hypothesis that no relaxation and no experimental misset intervene. The expected gain in the signal-to-noise ratio is quite clear for all spectra, except for that of sugar unit E, whose anomeric proton resonance is very close to those of units D and F. However, the overall reduction of acquisition time is large enough to be of practical interest.

The A matrix for Hadamard encoding with n = 7 would be obtained by removing the first row and the first column in H_8 (the ones with only +1 values) thus resulting in $v_j = 0.25$ $(1 \leqslant j \leqslant 7)$ and G = 4. Hadamard encoding might have been the best possible mixing scheme relying on amplitude modulation. However, in our particular case, this theoretical advantage is ruined by the need of exceedingly long selective pulses, whose duration is not compatible with relaxation and scalar couplings.

After the operating conditions were defined, the pulse sequence in Fig. 2a yielded the spectra in Fig. 3a. The estimate $\widehat{A}$ was obtained by integration of the doublets and scaled by dividing it by its maximum value, resulting in

$$v_{exp} = |\,0.54 \quad 0.31 \quad 0.33 \quad 0.90 \quad 1.18 \quad 0.70 \quad 0.26\,| \tag{12}$$

and G_{exp} = 2.18. The actual performance, although quite interesting, was slightly lower than theoretically expected. The reason might be found in pulse imperfection and relaxation effects. Spectra separation led to the seven isolated anomeric ^{1}H signals, as drawn in Fig. 3b.

The pulse sequence in Fig. 2b yielded the seven mixed 1D ^{1}H spectra in Fig. 4a. Their separation was carried out by matrix $\widehat{B}$, that was used to produce the separated anomeric signals in Fig. 3b. The result, in Fig. 4b, showed the seven nicely separated 1D ^{1}H NMR spectra of the seven sugar units in compound **1**. It should be noticed that the coupling constants of the anomeric

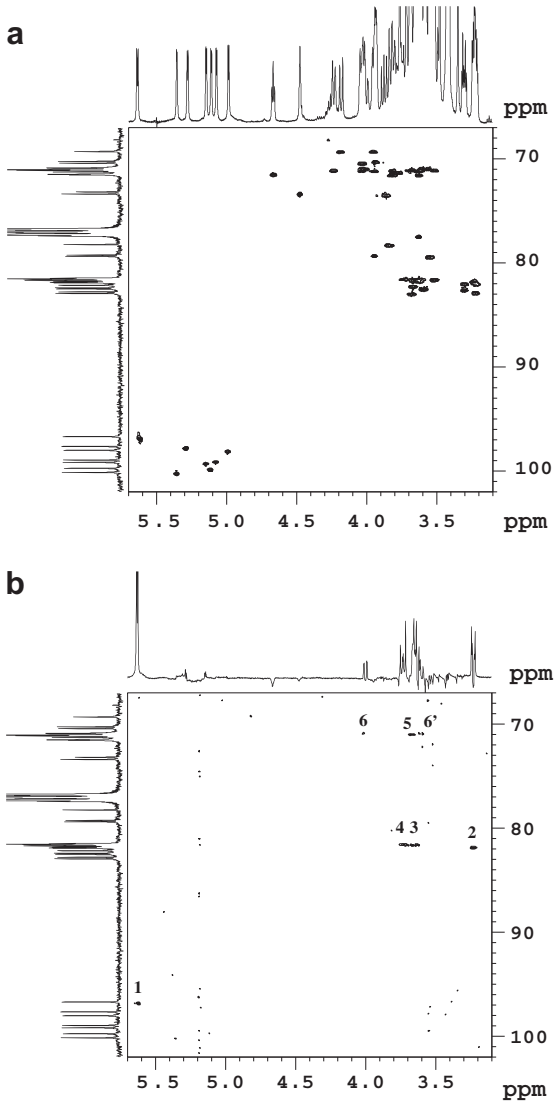

Fig. 6. (a) The HSQC spectrum of compound **1**. (b) The 2D-TOCSY-HSQC of sugar unit A. The complete set of 2D-TOCSY-HSQC spectra was obtained in 16 h and 10 min. (16 transients per t_1 value, 320 t_2 values). Inversion of ϕ_3 ($\pm y$) and of ϕ_5 separately result in ϕ_R inversion. Inversion of ϕ_4 does not change ϕ_R. $G_1/G_2/G_3/G_4 = 35/-35/\pm80/20$. The mixing matrix was computed by integration of the anomeric signals.

protons of the studied molecule are quite small (3–4 Hz range) which explains the low efficiency of the magnetization transfer between these protons and the rest of the spin systems. In spite of this limitation, sequences 2c and 2d were successfully run and led to two sets of seven 2D DQF-COSY and HSQC spectra. The non-selective spectra and the sub-spectra of sugar unit A are presented in Figs. 5 and 6. The two full sets of spectra for sugar units from A to G are provided as Supplementary Information. They allowed us to propose a full assignment of the ^{1}H and ^{13}C 1D NMR spectra of compound **1**.

4. Conclusion

Spin system selective 1D ^{1}H, 2D DQF-COSY and 2D HSQC NMR spectra were recorded in order to fully assign the ^{1}H and ^{13}C 1D NMR spectra of an asymmetrical β-cyclodextrin derivative. Instead of individually accessing the seven sugar anomeric protons by means of long multiplet selective pulses, only short region selective pulses were used. The simultaneously selected anomeric protons were differentiated by allowing their magnetization to evolve under the sole effect of the chemical shift interaction. In each experiment, the seven recorded spectra were linear combinations of the seven desired ones. The combination coefficients were measured and used to obtain almost perfectly separated sugar unit sub-spectra. This multiplexed acquisition scheme resulted in a time gain factor of about 2.

Acknowledgments

We thank Dr. Karen Plé for linguistic advice and Prof. F. Djeidani-Pilard for her assistance in the synthesis of compound **1**.

Appendix A. Supplementary material

Supplementary data associated with this article can be found, in the online version, at doi:10.1016/j.jmr.2010.06.005.

References

[1] R.R. Ernst, G. Bodenhausen, A. Wokaun, Principles of Nuclear Magnetic Resonance in One and Two Dimensions, Clarendon Press, Oxford, 1987.
[2] H. Kessler, S. Mronga, G. Gemmecker, Multi-dimensional NMR experiments using selective pulses, Magn. Reson. Chem. 29 (1991) 527–557.
[3] Ē. Kupče, T. Nishida, R. Freeman, Hadamard NMR spectroscopy, Prog. Nucl. Magn. Reson. 42 (2003) 95–122.
[4] J. Schraml, H. van Halbeek, A. de Bruyn, R. Contreras, M. Maras, P. Herdewijn, Hadamard 1D ^{1}H TOCSY and its application to oligosaccharides, Magn. Reson. Chem. 35 (1997) 883–888.
[5] V. Blechta, R. Freeman, Multi-site Hadamard NMR spectroscopy, Chem. Phys. Lett. 215 (1993) 341–346.
[6] V. Blechta, F. del Rio-Portilla, R. Freeman, Long-range carbon–proton couplings in strychnine, Magn. Reson. Chem. 32 (1994) 134–137.
[7] H. Bircher, C. Müller, P. Bigler, Improved sensitivity for the 2D analogue of the 3D HOHAHA-COSY experiment, Magn. Reson. Chem. 29 (1991) 726–729.
[8] J. Hadamard, Résolution d'une question relative aux déterminants, Bull. Sci. Math. 17 (1893) 240–246.
[9] C. Roumestand, C. Delay, J.A. Gavin, D. Canet, A practical approach to the implementation of selectivity in homonuclear multidimensional NMR with frequency selective-filtering techniques. Application to the chemical structure elucidation of complex oligosaccharides, Magn. Reson. Chem. 37 (1999) 451–478.
[10] S.W. Homans, Simplification of COSY spectra of oligosaccharides by application of a 2D analog of 3D HOHAHA-COSY, J. Magn. Reson. 90 (1990) 557–560.
[11] J.-M. Nuzillard, G. Massiot, Two-dimensional extensions of 1D HOHAHA experiments, J. Magn. Reson. 91 (1991) 380–385.
[12] O. Stephany, F. Dron, S. Tisse, A. Martinez, J.-M. Nuzillard, V. Peulon-Agasse, P. Cardinal, J.-P. Bouillon, (L)- or (D)-Valine tert-butylamide grafted on permethylated β-cyclodextrine derivatives as new mixed binary chiral selectors, versatile tools for capillary gas chromatographic enantioseparation, J. Chromatogr. A 1216 (2009) 4051–4062.
[13] D. Marion, K. Wüthrich, Application of phase sensitive two-dimensional correlated spectroscopy (COSY) for measurement of ^{1}H–^{1}H spinspin coupling constants in proteins, Biochem. Biophys. Res. Commun. 113 (1983) 967–974.
[14] R. Brüschweiler, C. Griesinger, O.W. Sørensen, R.R. Ernst, Combined use of hard and soft pulses for ω_1 decoupling in two-dimensional NMR spectroscopy, J. Magn. Reson. 78 (1988) 178–185.
[15] P. Berthault, H. Desvaux, B. Perly, Simple solutions to resolve extreme NMR spectral overcrowding using shaped pulses, Magn. Reson. Chem. 31 (1993) 259–265.
[16] Y. Zhang, B. Dausse, P. Sinaÿ, M. Afsahi, P. Berthault, H. Desvaux, Synthesis and NMR study of a heptasaccharide, epitope of the stage-specific embryonic antigen-1 (SSEA-1), Carbohydr. Res. 324 (2000) 231–241.
[17] H. Sato, Y. Kajihara, An unambiguous assignment method by 2D selective-TOCSY-HSQC and selective-TOCSY-DQFCOSY and structural analysis by selective-TOCSY-NOESY experiments of a biantennary undecasaccharide, Carbohydr. Res. 340 (2005) 469–479.
[18] H. Sato, K. Fukae, Y. Kajihara, 2D Selective-TOCSY-DQFCOSY and HSQC-TOCSY NMR experiments for assignment of a homogeneous asparagine-linked triantennary complex type undecasaccharide, Carbohydr. Res. 343 (2008) 1333–1345.
[19] H. Geen, R. Freeman, Band-selective radiofrequency pulses, J. Magn. Reson. 93 (1991) 93–141.